Available online at www.CivileJournal.org

Civil Engineering Journal

(E-ISSN: 2476-3055; ISSN: 2676-6957)

Vol. 9, No. 11, November, 2023

Durability Assessment of Sustainable Mortar by Incorporating the Combination of Solid Wastes: An Experimental Study

Mohammad Nadeem Akhtar [1*], Dima A. Husein Malkawi [2], Khaldoon A. Bani-Hani [1, 3], Abdallah I. Husein Malkawi [1, 3]

[1] *Department of Civil Engineering, Fahad Bin Sultan University, Tabuk, Saudi Arabia.*

[2] *Civil and Environmental Engineering Department, German Jordanian University, Amman, Jordan.*

[3] *On leave from Jordan University of Science and Technology, Irbid, Jordan.*

Received 20 May 2023; Revised 14 October 2023; Accepted 22 October 2023; Published 01 November 2023

Abstract

The excessive mining of high-quality river sand for cement sand mortar resulted in environmental impacts and ecological imbalances. The present study aims to produce sustainable mortar by combining solid waste such as desert sand, stone dust, and crumb rubber to fully replace river sand. In addition, replacing cement with silica fume helps reduce the environmental carbon footprint. The present research prepared three types of mortar mixes: natural dune sand mortar (M1), natural dune sand stone dust crumb rubber mortar (M2), and natural dune sand stone dust crumb rubber silica fume mortar (M3). The developed mortar samples were examined at ambient and elevated temperatures of 100°C, 200°C, and 300°C for 120 minutes. Furthermore, 3 cycles of 12 hours each at freezing temperature (-10° ± 2°C) and crushed ice cooling (0° to -5°C) were also tested. Results of the study showed an increment in compressive strength values in M1, M2, and M3 mortar mixes (up to 200°C). Later, an abrupt drop in the compressive strength was noticed at 300°C in all mixes M1, M2, and M3, respectively. The mix M3 combinations resist heating impacts and perform significantly better than other mixes M1 and M2. Also, M3 combinations resist the cooling effect better than M1 and M2. It can be concluded that the mortar mix M3 with desert sand, stone dust, crumb rubber, and silica fume combination is considered the best mix for both heating and cooling resistance. Hence, the developed sustainable mortar M3 combination can be utilized in all adverse weather conditions.

Keywords: Desert Sand; Stone Dust; Crumb Rubber; Silica Fume; Sustainable Mortar.

1. Introduction

River sand mining for construction substantially impacts the environment and the population thriving on the floodplain of rivers [1, 2]. The mining of sand on the banks of the Pearl River bed has accelerated the scouring, widened the channel area, and weakened the bridges and natural levees, according to Bendixen et al. [1]. China, India, Bangladesh, and other countries extract sand for construction activities, harming local hydrology and wildlife. According to Davis, landform development is a natural earth process that includes erosion and deposition of fine sediments along the river basin; extracting these fine sediments influences the ecology and shrinks the fertile land area for agriculture [3]. An estimate states that the global per-annum demand for natural river sand is approximately 50 billion tons, and it's increasing non-linearly [4]. This demand cannot be met by river sand alone. For this reason, the hourly demand is to search for alternatives to natural river sand as a construction material.

* Corresponding author: nakhtar@fbsu.edu.sa

http://dx.doi.org/10.28991/CEJ-2023-09-11-09

The natural dune sand (NDS) from the desert is a perfect option to replace the natural river sand in cement, sand mortar, and concrete. The planet is covered with desert sand, a prime example of the Arabian Peninsula and the Sahara Desert. Desert sand is the by-product of wind erosion; the continuum shifts in the dune sort and reduces grain size, which is inferior to river sand. Thus, it is not considered with the full replacement of river sand in cement sand mortar and concrete production. The NDS in cement sand mortar influences mortar properties and affects the strength and durability of cement sand mortar and concrete. The full replacement of NDS with river sand found a decrease in the NDS mortar's compressive strength, as studied by Seif & Sedek [5]. An abrupt decline in compressive strength was seen when more than 70% NDS was used. Another study by Abu Seif et al. [6] shows that up to 50% NDS is acceptable in concrete manufacturing. The workability and compressive strength were reduced in concrete at more than 50% substitution of NDS. Most recent studies showed that the partial replacement of natural river sand with recycled fine sand and the NDS combination performed well in design mix concrete [7–12].

In the recent past, several researchers have done a commendable job of utilizing solid wastes such as flyash, silica fume, recycled coarse and fine aggregates, stone dust, and blast furnace slag to replace natural materials [11, 13–19]. Industrial solid waste, such as crumb rubber (CR) and stone dust (SD), can also be replaced with natural materials for construction activities. In developed countries, the production rate of waste tires was calculated to be one tire per person. Waste tire production is expected to be 1.2×10^9 tons by 2030. About 4 billion tires are disposed of in landfills, and over 50% of waste tires worldwide are still discarded without recycling [10, 20]. Singapore and some Asian countries have done commendable jobs by recycling tire rubber to produce standard, high-performance concrete [21]. Bani-Hani & Senouci [22] investigate the performance of waste tire CR as an alternative aggregate for concrete pedestrian blocks. The CR concrete pedestrian blocks exhibited low compressive and flexural strengths. CR concrete blocks did not demonstrate the typical brittle failure, unlike plain pedestrian blocks. It exhibited ductile plastic failure and could absorb much plastic energy under compressive and flexural loads. A recent study by Akhtar et al. [7] demonstrated the acceptable performance of natural dune sand, stone dust, and crumb rubber concrete. An enormous amount of rock sludge and quarry dust from fine by-products is generated during mining, and these fine by-products in an open space cause significant environmental problem. Fine dust particles can accumulate in the air as suspended solid particles and hamper soil agricultural productivity by clogging up cation-anion exchange voids [23]. The results of the study by Ahmad Khan et al. [24] showed that the strength properties of cement mortar made by incorporating crushed SD were significantly higher than those of standard mortar.

Silica fume (SF) was used in the cement and concrete industry in the mid-20th century, in 1952, blended with OPC to enhance concrete strength and durability characteristics. The first commercial use of SF as a blender in a cement plant was made by Canadian cement manufacturers in 1982 [25]. According to ACI 234R-96 [26], companies sell SF-based cement containing 7–8% SF. Later, advancements were made to make it more sustainable by making combinations of SF percentages. A study described the potential use of cement containing 6-7% SF [27]. Recent studies on cement replacement with SF have shown improvements in concrete's hardened properties. Partial replacement of OPC with SF helps to reduce CO_2 emissions from the cement industry [9, 28, 29].

Past literature showed that NDS, CR, and SD waste materials replaced natural river sand in concrete manufacturing. It has also been disclosed that partial replacement of NDS, CR, and SD provides satisfactory concrete strength and durability results. The past review did not find much work in cement sand mortar by replacing natural river sand with a combination of NDS, CR, and SD. Experimental data also revealed that the studies on the durability characteristics of sustainable cement sand mortar are scanty. The NDS from the desert is a perfect option to replace the natural river sand with other waste materials such as SD and CR in cement sand mortar. This study fills the research gap and will open up unstudied potential by utilizing NDS, CR, SD, and SF in sustainable cement sand mortar. The present study attempted to refine the NDS by adding solid waste SD and CR to replace natural river sand. In addition, the partial replacement of OPC with SF was also studied. This experimental research studied the performance evaluation of sustainable mortar under heating and cooling temperatures. This work will open a new gateway and contribute mainly to its undiscovered potential. Furthermore, sustainable cement sand mortar will help reduce the natural river sand utilization in mortar. Finally, it will contribute to developing a sustainable environment and be another step towards green construction.

2. Experimental Investigation

2.1. Materials

The present research uses natural dune sand (NDS) from the desert as a reference sand material. In this study, stone dust (SD) and crumb rubber (CR) replaced the NDS, and silica fume (SF) was utilized as a partial replacement for ordinary Portland cement (OPC), as shown in Figure 1.

Figure 1. Materials (a) NDS, (b) SD, (c) CR, and (d) SF

2.1.1. Ordinary Portland Cement

The locally available batch of OPC has been utilized in the present study. The cement's physio-chemical parameters are as per the Gulf standard's specification (NO: 1914-2009).

2.1.2. Natural Dune Sand

Due to the dry atmospheric conditions on the Arabian Peninsula, a large portion of Saudi Arabia is covered in dunes, the desert's most significant geomorphological feature. The Aeolian process forms dunes and occupies the world's 8×10^5 km^2 area [30]. The dunes are predominantly confined on the eastern coast of the Arabian Peninsula. Thus, the heap of sand is mainly constrained to the far-flung areas of the Arabian Peninsula over the rocks of the Precambrian era [31].

2.1.3. Stone Dust

Crushed stone is a form of aggregate used in the construction industry, typically produced by mining several rocks such as limestone, dolostone, granite, traprocks, basalt, sandstone, and sometimes marble, based on availability. The quarrying of stone blocks is the primary source of dust production, crushed into small chips using a crusher of sizes like 6 mm, 20 mm, 45 mm, or, as per requirement. Many rock types are used to make crushed stones; sometimes, these crushed stones are classified based on the color of dust produced while crushing/mining, such as black stone dust and red stone dust. The rock types in this category include igneous, metamorphic, and sedimentary rocks. In the present study, locally available red stone dust replaced the NDS as fine aggregate in sustainable mortar.

2.1.4. Crumb Rubber

Crumb rubber is produced after crushing off automobile tires as scrap, mainly in industries. They are mashed to powder state up to 40 mesh size during the process, and all other tire components, like steel, fabric, etc., are removed up to 99%. This study uses CR as a fractional substitution of NDS at a threshold value of 5% in the mixes M2 and M3, respectively.

2.1.5. Silica Fume

In the present research work, SF partially replaced OPC. The most revolutionary concrete additive that has been developed in recent times is microsilica fume. The microsilica fume has two times more bulk density, making it distinct from other supplementary mixes, and poses many benefits. It is dustless, sleeky, even, lump-free, and less dense.

2.2. Methods

The detailed flow chart of the present research work methodologies is presented in Figure 2. The study aims to develop a sustainable sand mortar by incorporating waste materials such as NDS, SD, CR, and SF. The standard test method mentioned in Figure 2 evaluated the physicochemical properties of utilized materials. After evaluating the physicochemical characteristics, the design mix was done as per the standard criterion described in the flow chart in Figure 2. Finally, three types of sustainable mortar were prepared to evaluate the durability characteristics under different parameters as described in the flow chart in Figure 2.

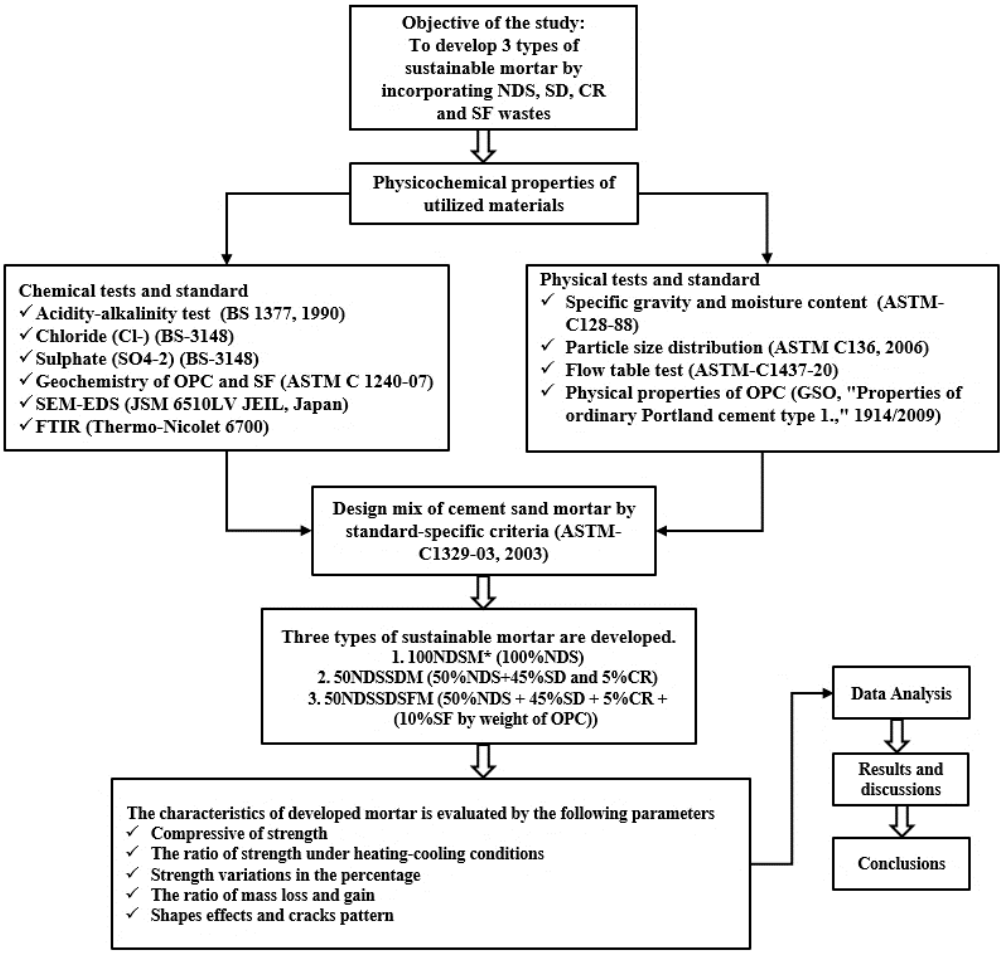

Figure 2. The detailed research flow chart

2.2.1. Chemical Properties for SD and CR

The physical and chemical parameters of SD and CR are incorporated in this study by following the same methods used by Akhtar et al. [7]. Before commencing experimental analysis, it has been confirmed by the researcher that all instruments are clean, tested, and calibrated to maintain accuracy and precision in data. The SD and CR specimens were baked in an oven for 120 minutes at 110°C. The specimen's pH (acidity-basicity index) reading was measured by Systronic µ pH System 361 using a calibrated buffer tablet pH meter. The Agilent ATR module of Cary 630 FTIR determined the sample's FTIR spectra. These spectra can determine the amount of light absorbed by the samples at a wavelength within a specific band range of 600-4000 cm^{-1}. It also helps to depict whether any unwanted material (steel, fabric) is present in the samples. The surface morphology was scanned in an Electron Microscope (SEM) with elemental quantification using Energy-Dispersive X-rays (EDX) spectroscopy.

2.2.2. Geochemistry of OPC and SF

OPC Type 1 confirms the SASO/GSO 1914/2009 chemical properties in Table 1. The SF chemical properties were assessed as per the standard ASTM C1240-20 [32] mentioned in Table 2.

Table 1. Chemical properties of OPC Type 1

Chemical Parameter	Obtained Values	Specified Limits
SiO_2	20.24%	Limit not specified
Al_2O_3	5.24%	Limit not specified
Fe_2O_3	4.19%	Limit not specified
Cao	62.36%	Limit not specified
MgO	2.86%	5% Maximum
SO_3	2.91%	3% Maximum
Loss of Ignition (LOI)	1.10%	3% Maximum
Insoluble Residue (IR)	1.22%	1.5% maximum
Lime Saturation Factor (LSF)	0.92%	0.66-1.02
Tricalcium Aluminate (C_3A)	6.79%	Limit not specified

Table 2. Chemical properties of CSF-85

Chemical Parameter	Obtained Values	Specified Limits
SiO_2	88.53%	85% min
Moisture Content	0.38%	1.0% max
LOI	2.79%	3.0% max
Al_2O_3	0.60%	-
Fe_2O_3	1.73%	-
CaO	0.72%	-
MgO	1.27%	-
SO_3	1.31%	-
Accelerated Pozzolanic Activity	120.00	105% min
Specific surface	>18	15-30 m^2/g

2.2.3. Hydrochemistry

The chemical test aims to know the pH values for concrete and mortar as a primary yardstick to know the concrete and mortar resistance towards chemical reagents. Therefore, before performing this test, the water sample is first tested and, according to BS 3148 [33], contains no other reactant. Thus, water sample becomes suitable for testing concrete and mortar mixes and other construction tasks. The values obtained from the test are found in the standard ranges advised by BS 3148 [33] and are shown in Table 3.

Table 3. Curing water index

Parameter	Observations	Ranges	Standards
pH	7.2	6.9-9.2	BS-3148
Sulphate (ppm)	222.0	<1000	BS-3148
TDS (ppm)	358.0	<2000	BS-3148
Chloride (ppm)	94.0	<500	BS-3148

2.2.4. Specific Gravity and Moisture Content

The specific gravity of any component has a considerable part in devising the plan for concrete and mortar mixes. In this research, parameters such as saturated dry surface (SSD), bulk, apparent specific gravity, and moist soaking tendency were calculated as per ASTM C128-22 [34] and for OPC, according to GSO 1914/2009 [35]. It is imperative to remark that the SD, CR, and SF show the highest water absorption than the NDS sample while having negligible specific gravity. Table 4 shows experimental values of NDS, SD, CR, and SF, and Table 5 records the physical parameters of OPC.

Table 4. Physical properties of NDS, SD, CR, and SF

Physical Parameters	Values			
	NDS	SD	CR	SF
Specific gravity (SSD)	2.626	2.591	-	-
Specific gravity (bulk)	2.584	2.321	-	2.2
Specific gravity (apparent)	2.696	3.177	-	-
Percentage water absorption	1.626	11.61	2.97	26.08

Table 5. Physical properties of OPC

Physical Parameter	Obtained Values	Specified Limits
Fineness (cm^2/gm)	3546	2800 (Min)
Setting time (Minutes)		
Initial	146	45 (Min.)
Final	233	375 (Max.)
Soundness		
(a) Le Chatelier (mm)	1.00	10.0 (Max.)
(b) Autoclave (%)	0.05	0.80 (Max.)
Air content (%)	7.90	12.0 (Max.)
Compressive Strength		
3 days	24	12 (Min.)
7 days	29	19 (Min.)
28 days	37	28 (Min.)

2.2.5. Particle Grading

The sieve analysis was done for size distributions NDS, SD, CR, and SF by ASTM C136-06 [36]. First, the data obtained is converted into a cumulative percentage of passing the materials versus standard sieve; later, data was plotted in a log scale, as shown in Figure 3. From Figure 3, the grain size gradation curves of NDS and CR were between the upper and the lower limit, which satisfies the requirement of the ASTM-C136-06 standard. On the other hand, the particle size distribution curve of SD lies very close to the lower limit values, but SF was out of the range. Therefore, it indicates that the SF is a comparatively finer particle.

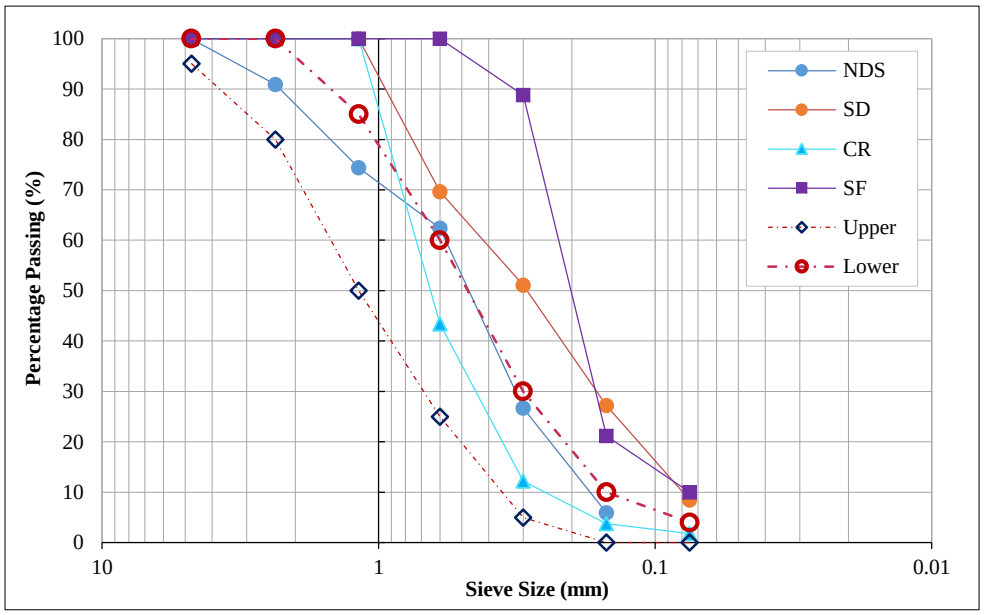

Figure 3. Sieve analysis results along with upper and lower limits

2.2.6. Flow Table Test

Samples were tested to calculate the quantity of water needed to measure the strength test of the cement. It also gives an idea of the workability of sustainable cement sand mortar. The mortar mixtures were prepared and flow-controlled [37, 38]. The waste materials were mixed with cement to prepare sustainable cement sand mortar. As calculated in Table 4, the SD, CR, and SF water absorption values were very high. Several trail mixes were done to achieve the desired flow values of mortar mixes M1, M2, and M3. The w/c ratio and admixture doses were adjusted against the standard flow, ranging from 105% to 115%.

The temperature and relative humidity measured in the experiment were 25 ± 2°C and 60 ± 5 %, respectively. A specific amount of cement, other materials, and water are mixed to make mortar and notice flow with 25 drops in 15 seconds**.** In the non-viscous mortar, a subsequent rise of inflow in the average base diameter of the mortar mould was measured in a minimum of 4 diameters at similar distance intervals (which is stated as a percent of the original diameter base). The values of flow were measured by Equation 1.

$$\text{Flow} = \frac{D_{avg} - D_o}{D_o} \times 100 \quad (1)$$

where D_{avg} is Average base diameter, and D_o is original base diameter of the casing.

All necessary precautions were taken during the experimental investigation. The test material for each mix of the test specimen was mixed separately. Compaction was sufficient in each mix to ensure the mould was filled evenly. The flow % in mortar, w/c ratio, and admixture amounts are given in Table 6. The experimental setup of the flow test is shown in Figure 4-a prepared sample Figure 4-b measuring diameter.

Table 4. Flow (%) of prepared mortar

Mix Mortar	Flow (%)	Specified flow (%)	W/C ratio	Admixture by weight of cement
100NDSM	110	105% to 115%	0.60	0.3
50NDSSDM	115	105% to 115%	0.90	0.7
50NDSSDSFM	115	105% to 115%	1.10	0.9

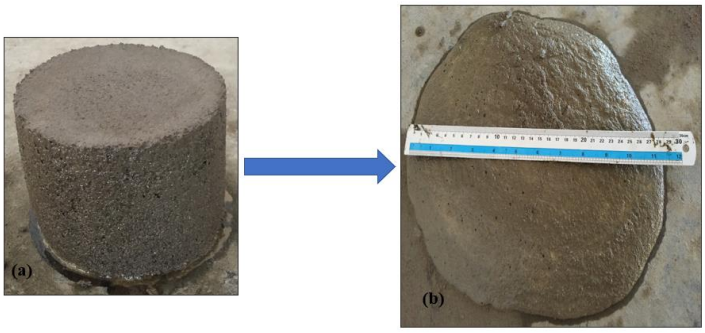

Figure 3. Experimental setup of flow test: (a) prepared sample (b) measuring diameter

2.2.7. Design Mix Mortar

The work has been carried out in three phases: the first Phase, the second phase, and the final third Phase. In the first phase, a reference sample was made by mixing (100%NDS) for natural dune sand mortar (M1). In the second phase, 50%NDS was replaced with 45%SD and 5%CR to produce a natural dune sand stone dust crumb rubber mortar (M2). In the third Phase, OPC was substituted with SF by (10% of the weight of OPC). The final mix was completed in the composition of SD, CR, and SF and designated as natural dune sand stone dust crumb rubber silica fume mortar (M3) with (50%NDS + 45%SD + 5%CR + (10%SF by weight of cement)) respectively. Finally, the prepared mortar samples of three different mixes (M1), (M2), and (M3) were tested after 28 days of curing in axial compressive strength at ambient temperature (AT) and higher temperatures of 100°C, 200°C, and 300°C for 120 minutes. Furthermore, the compressive strength of mixes (M1), (M2), and (M3) were also evaluated after freezing and the crushed ice-cooling cycle for 36 hours.

The three mortar mixes, (M1), (M2), and (M3), in the ratio of (1:4) cement-sand by volume, were prepared. The amount of water in the mixes (M1), (M2), and (M3) was calculated at 229.82 kg/m^3, 344.74 kg/m^3, and 421.34 kg/m^3, respectively. The other mixed quantity of discrete mixes is shown in Table 7.

Table 5. Mortar mix proportions

Mix	Cement (%)	NDS (%)	SD (%)	CR (%)	SF (%)	W/C ratio	Admixture by weight of cement
100NDSM*	100	100	-	-	-	0.60	0.3
50NDSSDM	100	50	45	5	-	0.90	0.7
50NDSSDSFM	90	50	45	5	10	1.10	0.9
100NDSM* Control mix							

The research relies on the judgment obtained from past studies. The observation of past studies took the replacement ratio of SD 45%. The study by Suman et al. [39] successfully replaced natural river sand with SD up to 50% without compromising mechanical properties. Other studies [7, 40-42] showed the partial and full replacement of SD with natural sand in concrete and mortar. The other waste materials, CR and SF, were optimized with a control mix of M1, and the optimal value of 5% and 10% was used in this study.

The mortar performance was measured using the flow table test for the recommended flow value of 105 to 115% by ASTM C1437-20 [37]. The water content required for workability was determined on a trial-and-error basis for each mix. For each mix, the results are based on the trial values adjusted by the admixture's doses shown in Table 7.

In the present study, 54 mortar cubes with a dimension of 100 mm × 100 mm × 100 mm were made. After preserving the specimens for 28 days, the mortar strength is measured at ambient and elevated temperatures. First, the mortar cube samples were prepared and preserved in the laboratory. Then, three prepared samples were tested from each mix at AT, 100°C, 200°C, 300°C, freezing, and ice-cooling cycle (54 samples). For freeze, the ice-cooling cycle was continued for 36 hours for 3 cycles, 12 hours each at (-10 ± 2°C) in an automatic freezer and (0 to -5°C) in crushed ice. The test started from the ambient temperature, and the temperature dropped linearly to (-10 ± 2°C) for the freezer and again increased back to ambient temperature after 12 hours of waiting. The temperature meter was fixed on the opposite sides of the ice-cooling box, and temperatures were observed (0 to -5°C) throughout the cycle. The variation in the temperature is due to the melting of ice, and the temperature of the test box was measured throughout the cycle to avoid further fluctuation. The systematic diagram of the experimental setup is shown in Figure 5. The mortar cube of 100 mm samples was tested under a motorized machine (C056A) of 2000 kN, maximum capacity with an Auto-technical regulator. The primary strength indicator of concrete and mortar was applied to measure the compressive strength of samples ASTM C39/C39M-01 [43].

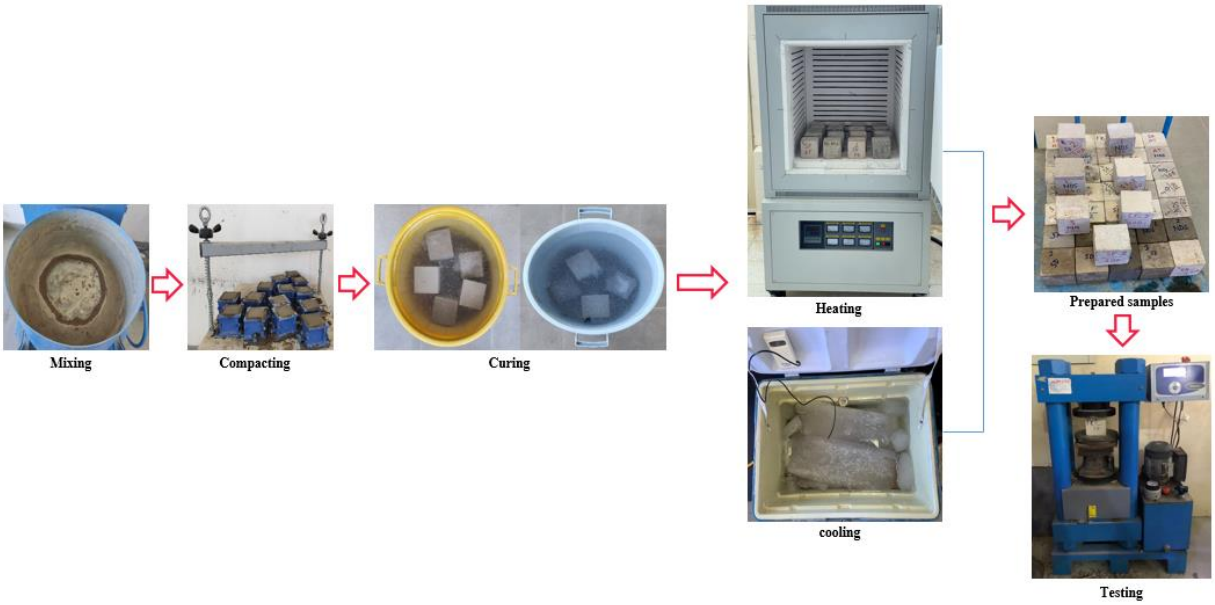

Figure 4. Systematic diagram of the experimental setup

3. Results and Discussion

3.1. Chemical Analyses

In this study, solid waste stone dust (SD) and crumb rubber (CR) was taken from the same batch utilized by Akhtar et al. [7] to evaluate the performance of sustainable sand concrete at ambient and elevated temperature.

3.1.1. Acidity-alkalinity Test

The durability of cementitious compound concrete increases with increased pH [44, 45]. For example, the pH for the CR sample is 7.36, and the SD was 7.03; it was observed that pH values of SD and CR in the range of 6 and 8 make them act as neutral fillers [46, 47]. To avoid contamination or reaction of the concrete and mortar, the samples were washed carefully with distilled water for about 24 hours before resuming a pH test. As a result, the pH values of the samples CR and SD were 7.36 and 7.03, respectively.

3.1.2. FTIR Analysis

FTIR spectroscopic analysis is the quality control technique for evaluating industrially manufactured materials. FTIR is used to determine the characterization of the functional group present in SD and CR. The SD FTIR spectra are represented by a band range of 1003 cm-1$^{\lambda}$ showing Silica-Oxygen-Silica, Silica-Oxygen str., and at 778 cm-1 $^{\lambda}$ the observed band is Silica-Oxygen str, Silica-Oxygen-Alumina str (Al, Mg) -Oxygen-Hydrogen Aluminium-Oxygen-(Magnesium, Aluminium) str. FTIR spectrum of dune restricts a soil-like material (inorganic components such as silica) used in the cement industry. However, the CR's FTIR spectra represent Carbon-Hydrogen's widening vibrations of –Carbon=Carbon at the 2990 cm-1 band range. The observed band wavelength at 1424 cm$^{-1\,\lambda}$ denotes the band oscillations of the Carbon-Hydrogen (=CH_2) functional class. The spectrum of CR indicates the presence of Carbon=Carbon for isoprene. However, the carbon-based constituent in CR gets deformed at higher temperatures. Therefore, a lower percentage of CR is recommended. The FTIR spectrum of SD and CR are presented in Figure 6.

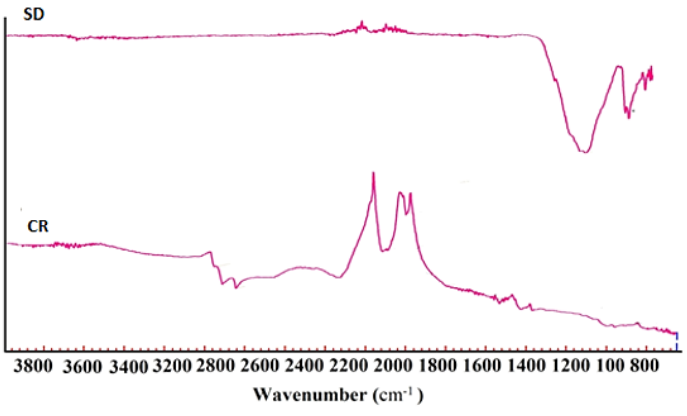

Figure 5. FTIR of SD and CR

3.1.3. SEM-EDX Analysis

To investigate the surface texture, shape, and elemental analysis of individual grains present in SD and CR, Electron Microscope scanning (SEM) was carried out. For this purpose, around 1g of the powdered sample was allowed to pass through a sieve of 75 µm mesh and positioned on the stub of the instrument, followed by an activated vacuum chamber with an electron beam. High-resolution SEM images are attained through a backscattered e$^-$released from the model. It is detected that the SD specimens are bulky in size, coarse with irregular outlines, and the texture of the surface is rough, whereas CR is latex, which shows a smoother surface in the SEM images Saxena et al. [48]. The specimen's elemental credentials and chemical arrangement were made using energy-dispersive X-ray studied by Dehdezis et al. [49]. The binary plot of SD depicts elemental components such as Mg, Si, Fe, Al, K, C, and O, whereas specimens of CR have additional peaks Ti. Figure 7 shows SEM images and EDX analysis for specimens SD and CR.

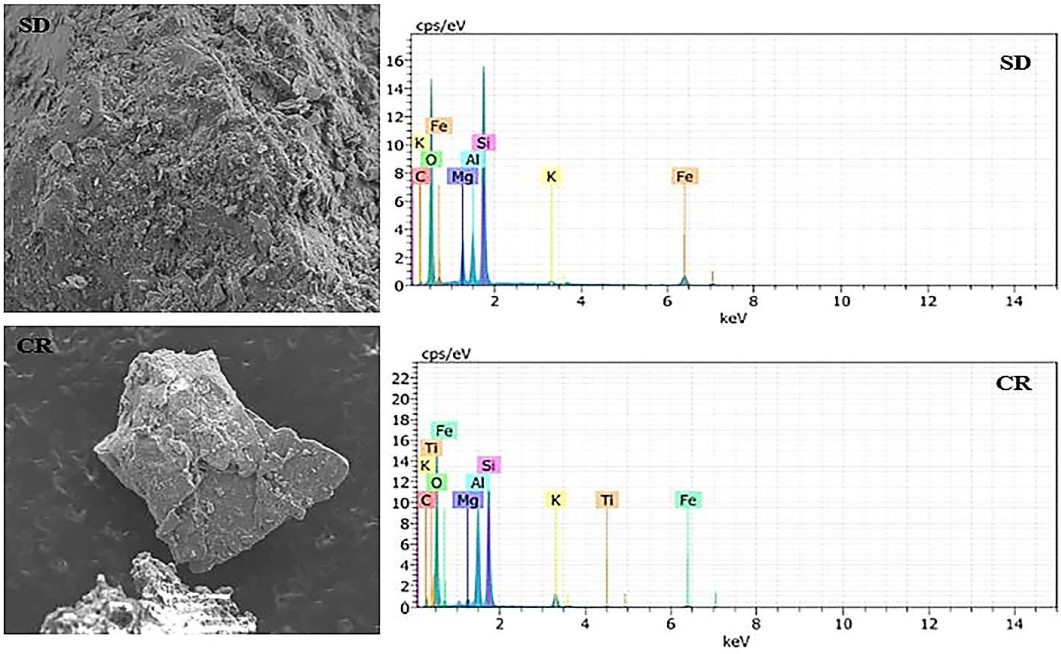

Figure 6. SEM images and EDX analysis for specimens SD and CR

3.2. Strength Characteristics

3.2.1. Compressive Strength of Developed Sustainable Mortar

In the present research work, the design strength was expected to be 12.4 MPa, 5.2 MPa, and 2.4 MPa of cement sand mortar Type S, Type N, and Type O specifications as per standard ASTM C270-19ae1 [50]. The prepared samples were well-maintained under 28 days of curing at 23 ± 2°C. Cement sand mortar cement must fulfill the criterion set by ASTM C1329-03 [51]. The compressive strength characteristics of developed sustainable mortar under heating-cooling conditions are shown in Figure 8. The mortar strength was evaluated at AT and elevated temperatures of 100°C, 200°C, and 300°C, respectively. The strength was also tested at freezing temperatures (-10 ± 2°C), and the ice-cooling temperatures were (0 to -5°C). In the first phase, the compressive strength at ambient temperature of the mixes $M1_{AT}$, $M2_{AT}$, and $M3_{AT}$ were 5.333, 5.288, and 8.690 MPa, respectively.

The compressive strength of ($M3_{AT}$) combination was the highest (8.690 MPa). All mixes achieved the design strength and fulfilled the requirements of Type N and Type O. In the first phase, mixes failed to reach the required target strength of Type S. The compressive strength values of the control mix ($M1_{AT}$) were found to be 5.333 MPa, attaining about 60% of the target strength of Type S. In the second phase mix ($M2_{AT}$), in which NDS has been replaced by 50% with (45% SD + 5% CR), the compressive strength has slightly decreased with a value of 5.288 MPa. In the third and final phase, 10% OPC was replaced by SF ($M3_{AT}$). When SF was added, the highest compressive strength, 8.690 MPa, was evaluated in the combination of the third phase. As a result, the compressive strength was decreased by 0.84 % in ($M2_{AT}$) and increased by 62% in ($M3_{AT}$) compared to the control mix of ($M1_{AT}$). In the third phase, a significant increase in compressive strength ($M3_{AT}$) with SF combination is attributable to the adhesive properties of SF, SD, and OPC gel. The OPC reacts with SF, and CH produces extra C-S-H in other pore spaces besides hydrated cement. Even if SF did not react chemically, the micro-filter effects improved mortar strength samples considerably.

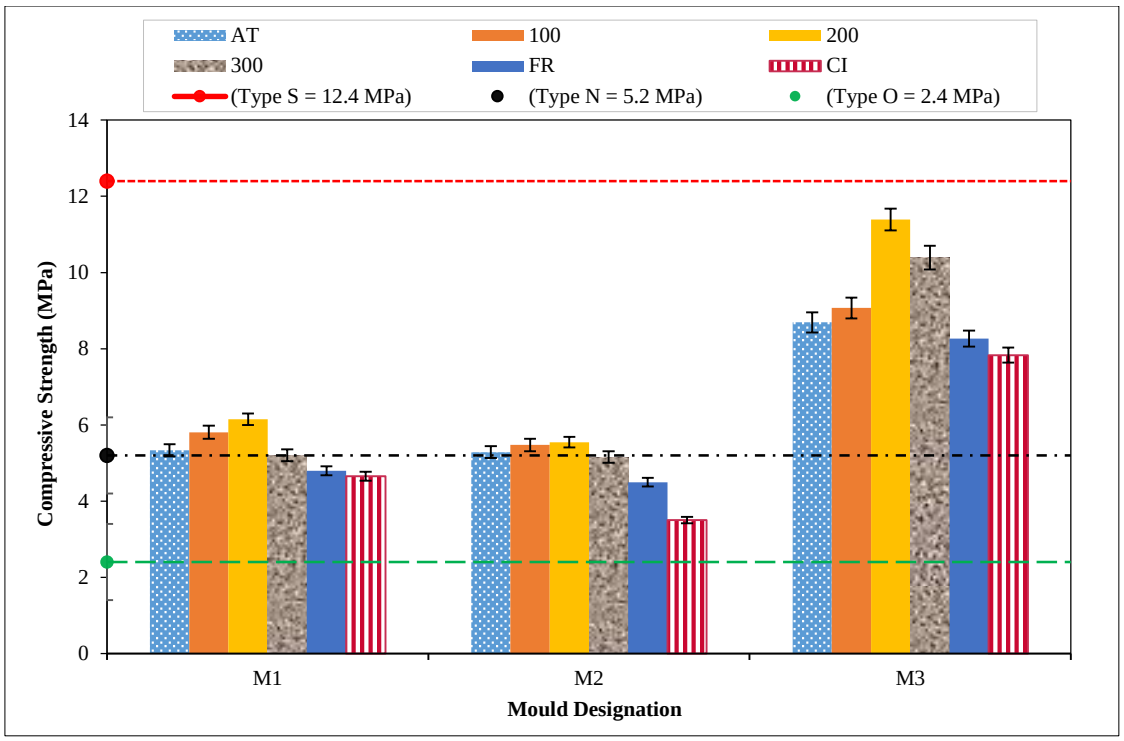

Figure 7. Compressive strength evaluation between mixes M1, M2, and M3

The rise in fire accidents has grabbed the attention of researchers to know the concrete and mortar behavior at high temperatures. Concrete and mortar are essential building materials that can maintain their properties at high temperatures. The latest research has shown variations in concrete and mortar strength with temperature, composition, aggregate types, the water/cement ratio, and supplements of OPC [52, 53]. In the second stage, the compressive strength was evaluated at higher temperatures of 100^{0}C, 200^{0}C, and 300^{0}C, respectively. The compressive strength of the mixes (M1, M2, and M3) increases up to 200^{0}C. The M1, M2, and M3 strengths increase because of water evaporation from the admixture surface and internal pore spaces of the mortar samples. At 300^{0}C, a sudden decline in compressive strength was recorded. It could be due to breaking the bond of some aggregates whose composition is siliceous. Even at 300^{0}C, the compressive strength of the mix M3 is found to be higher than the control mix M1. It happened due to the high thermal resistance of crumb rubber when mixed with silica fume, as studied by Fadiel et al. [54]. Several recent studies [7, 9, 55, 56] revealed the performance of design mix concrete made by incorporating solid wastes such as recycled aggregates, stone dust, and silica fume combinations at elevated temperatures. They found an increment in the compressive strength up to 200^{0}C. A recent study by Akhtar et al. [7] on design mix concrete with NDS and recycled crushed sand combination disclosed the exact behavior of concrete samples up to 200^{0}C. The studies for directly comparing cement sand mortar at elevated temperatures are unavailable. However, the present study's results align with the published studies on design mix concrete discussed above.

Figure 8 shows the mean compressive strength of 3 samples from each mix. Figure 8 confirms that the compressive strength of tested specimens illustrates a linear progression at all temperatures about standard mixes of type N and Type O. Figure 8 depicts that the configuration M3 is the best outcome at AT and elevated temperatures. A maximum fall in compressive strength in all three mixes is observed when the samples are exposed to crushed ice-cooling (CI).

3.2.2. Ratio of Strength under Heating-cooling Conditions

The residual compressive strength ratio of heating-cooling to the ambient temperature is shown in Figure 9. The maximum relative strength obtained in the developed mortar mixes M1, M2, and M3 at 200^{0}C was 1.153, 1.048, and 1.31, respectively. The minimum relative strength under ice-cooling conditions for the mixes M1, M2, and M3 were found to be 0.872, 0.662, and 0.901, respectively. In both conditions, the maximum values of developed sustainable mortar were obtained in M3, and the minimum was in M2. It shows that the compressive strength under variable temperatures is mutually reciprocal up to 200°C. However, in M1, the value is 1.153, although an increase of compressive strength at 200^{0}C is only about 15% higher than ambient temperature. In other mixes, such as M3, the highest increment is about 30%, and M2 has the lowest, about 5%. All the samples were significantly reduced when put under a crushed ice-cooling box (0 to -5°C) for 36 hours. The decreased compressive strength of sustainable mortar mixes M1, M2, and M3 was approximately 12%, 33%, and 10%. An abrupt decline in the strength was observed in all mixes at 300^{0}C. Under the automatics freezer at (-10 ± 2°C), the sustainable mortar mixes M1, M2, and M3 showed a 10%, 15%, and 5% reduction. It did not show any significant variation. The mix designation M3 gives excellent performance regarding heating cooling effects on sustainable mortar samples. Based on the practical outcomes, it is

revealed that SD and CR, along with SF, achieved satisfactory results in heating cooling effects on developed sustainable mortar. Hence, SF up to 10% is suggested for use in sustainable cement mortar.

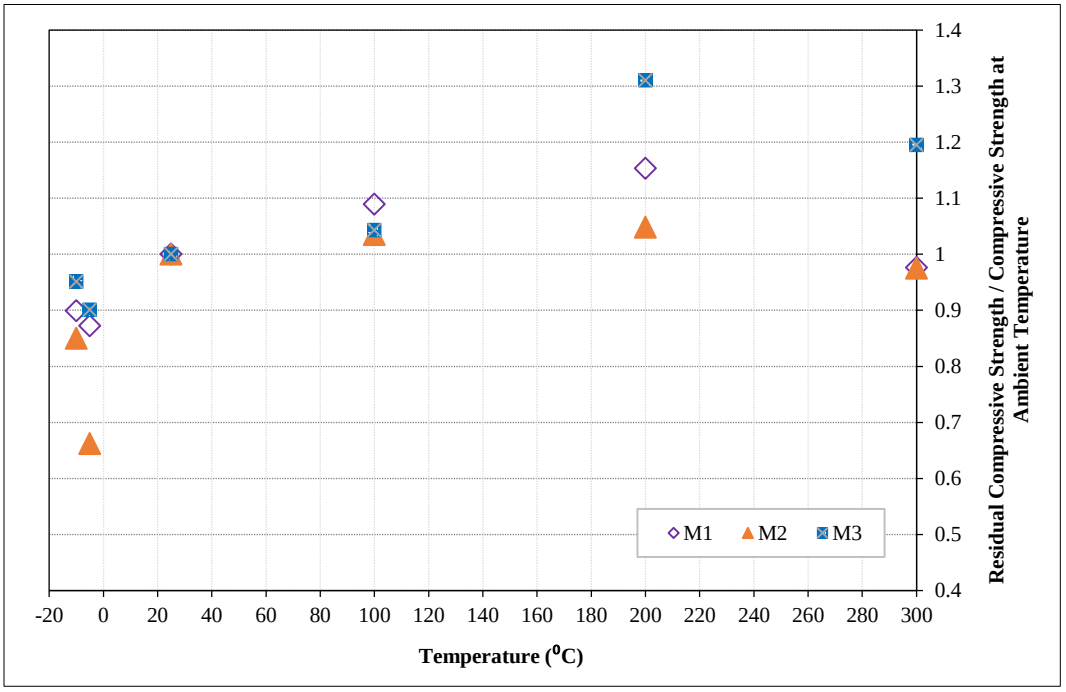

Figure 8. Comparison ratio of strength under heating-cooling conditions

3.2.3. Strength Variations

The variation in the compressive strength of developed sustainable mortar mixes M2 and M3 compared to the control mix M1 is shown in Figure 10. It can be seen from Figure 10 that mix M3 shows a substantial rise in strength in all parameters, such as AT, high temperatures, freezing, and ice-cooling. The reduction in the percentage of strength declines for the mix M2 at AT, 100^{0}C, and 200^{0}C compared to control mix M1. In the mix, M3 of (50%NDS + 45%SD + 5%CR + (10%SF by weight of OPC)) was found to have a negligible difference at 300°C. The rise in the compressive strength of M3 has the highest value of about 32% under ice-cooling. The average compressive strength of standard mortar samples should reach the value of (Type S) 12.4 MPa, (Type N) 5.2 MPa, and (Type O) 2.4 MPa, as suggested by ASTM-C-270 [50].

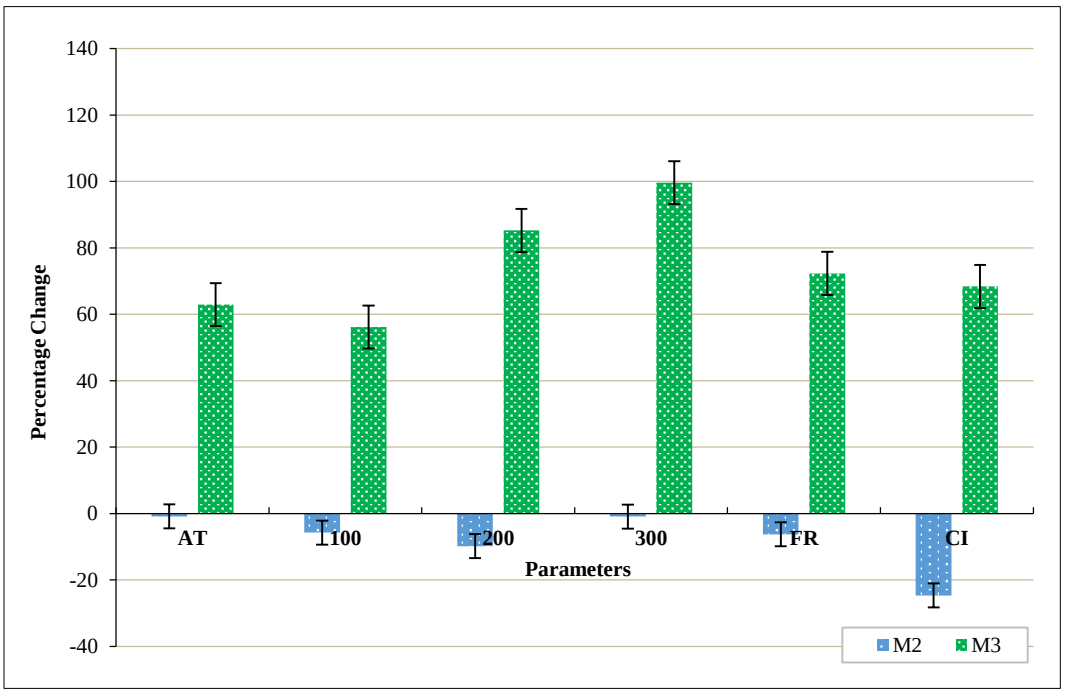

Figure 9. Change of strength compared to control mix 100NDSM

The mixes of M2 and M3 samples attained 85% of the design strength of Type N and Type O, respectively. For the present study, developed sustainable mortar mixes were found to be less than 12.4 MPa of Type S standard cement sand mortar requirement set by ASTM C270-19ae1 [50]. The mix M3 shows satisfactory results, and the highest value was reached at about 11.4 MPa, which is very close to the target value of 12.4 MPa of Type S standard cement sand mortar ASTM C270-19ae1 [50]. The M3 mix has almost identical performance in compression compared to M1 and M2. It has reached Type N and Type O standard cement sand mortar conditions and closely matches Type S of 12.4 MPa recommended by ASTM C270-19ae1 [50].

3.3. Ratio of Mass Loss and Gain

The ratio of mass loss and the gain developed sustainable mortar mixes M1, M2, and M3 are presented in Figure 11. At elevated temperatures of 100^0C, 200^0C, and 300^0C, samples from each mix were kept in the electric oven for 120 minutes. The change in mortar mass is mainly attributed to after-heating. The freezer and ice-cooling samples were put in a deep freezer and crushed in an ice-cooling box for 36 hours to know the cooling effects. Mortar samples were exposed to the freezer (-10 ± 2°C) and crushed ice-cooling box (0 to -5°C) for 36 hours in 3 cycles of 12 hours each. The samples were taken from the freezer and crushed ice-cooling box and then exposed to room temperature before testing. The mass loss ratio, β, was calculated using Equation 2.

$$\beta = \frac{m_1 - m_o}{m_o} \times 100\% \quad (2)$$

where m_o is the samples' original mass before heating and m_1 is the residual mass after the heating and cooling. Figure 11 represents the mass loss and gain ratio. The average value of β for all three samples is taken for interpretation. In the reference mix M1, the mass loss has lowered than M3. The rise in the rate of water loss from M3 samples is detected, perhaps due to the absorption of a higher amount of water absorption by SD and SF, 11.61% and 26.08%, presented in Table 4. The mass-loss rate is directly proportional to the elevated temperatures. Figure 11 shows that the higher the temperature, the more significant the mass-loss rate. The mass loss trend at 100^0C and 200^0C in the mixes M1 and M3 were higher than M2. When the temperature reached a maximum of 300^0C, the mass loss in the mixes M1, M2, and M3 was 6.182%, 8.411%, and 8.903%, respectively. The trends at 300^0C have satisfied that water loss from the samples corresponds to the water absorption values of mixing materials such as SD, CR, and SF, respectively.

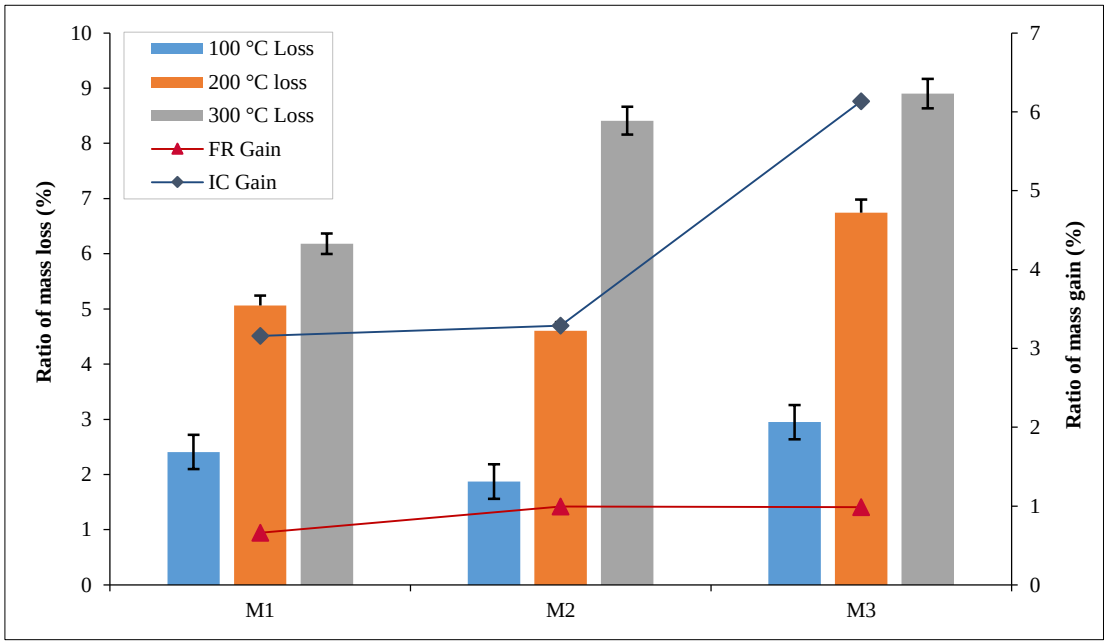

Figure 10. The mass loss and gain ratio

The mass loss rate in design mix concrete was measured by Pathak & Siddique [57]. It was found that between 200°C to 300°C, mass loss was higher than between 27°C to 200°C. Due to the structurally present H_2O molecule loss which was held in the structure, released from the C-S-H, $(Al(OH)_3$, and $(3CaO \cdot 2SiO_2 \cdot 3H_2O)$ when subjected to higher temperatures, which makes them unstable and therefore get escaped from the tested concrete samples. It is stated by Fares et al. [58] that when concrete is subjected to 300^0C, about 70% of the water evaporates from it. In a recent study by Akhtar et al. [7] on design mix concrete with NDS, SD, and CR combination, the mass loss shows a similar disparity at 100^0C, 200^0C, 300^0C, and 400^0C. It has been concluded by the present study that 300°C is a critical temperature, and the results were in line with published studies on design mix concrete.

The ratio of mass gain is observed in the samples kept in the freezer and crushed ice-cooling box. The water absorption value increases in parallel to the decrease in temperature value. In the present study, the developed sustainable mortar mixes are exposed (-10 ± 2°C) for the freezer (FR) and (0 to -5°C) for crushed ice-cooling (IC). The highest ratio of mass gain was obtained in mix M3 compared to the other mixes, M1 and M2, in the samples under the crushed ice-cooling box. Mass gain increases due to increasing void structure when temperature decreases in crushed ice water. No noticeable gains were seen in the samples under the freezer. The graph for the mean ratio of mass loss and gain values is presented in Figure 11.

3.4. Shapes Effects and Cracks Pattern

3.4.1. Shape Effects

After exposure to varying temperatures of developed sustainable mortar mixes, it has been observed that mortar specimens get deformed and their appearance after exposure to varying temperatures. Figures 12 to 14 show the sample observation of the sustainable mortar mixes M1, M2, and M3 at 100°C, 200°C, 300°C, FR, and IC, respectively. There was no difference in color observed at 100°C compared to AT. However, when the temperature reaches 200°C, the color of mortar specimens turns from light grey to dark grey, further increasing the temperature to 300°C; an unexpected change was noticed from dark grey solid to pale yellow. It could be due to the expansion and widening of the space lattices, which allowed light to reflect and the chemical decomposition of hydrates

Figure 11. Failure mode of 100NDSM samples at (a) 100, (b) 200, (c) 300, (d) FR, and (f) IC

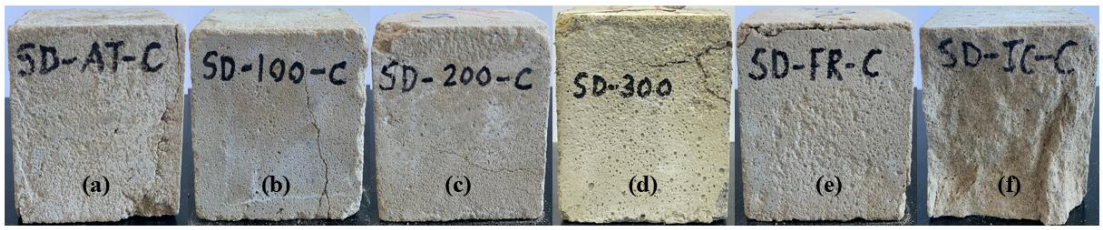

Figure 12. Failure mode of the 50NDSSDCRM samples at (a) 100, (b) 200, (c) 300, (d) FR, and (f) IC

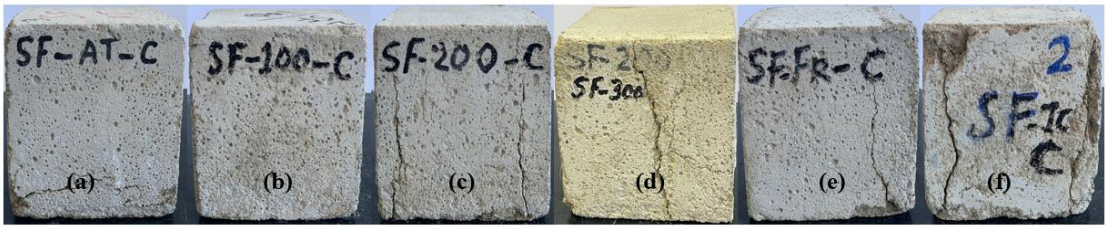

Figure 13. Failure mode of the 50NDSSDCRSFM samples at (a) 100, (b) 200, (c) 300, (d) FR, and (f) IC

After 36 hours, samples were taken from the freezer and ice-cooling box and then exposed to room temperature. The samples under the crushed ice-cooling box showed severe damage on the surfaces. The color of the samples changes to a light brown color, which may be due to the further hydration of the mortar composite.

3.4.2. Crack's Pattern

The typical cracks in the developed sustainable mortar mix M1, M2, and M3 are shown in Figures 12 to 14. The cone & split and columnar fractures with nerve-like crevices were observed at 100^0C and 200^0C. The failure mode of samples displays an almost regular pattern of mortar. Vertical splits develop when the load is maximized on the mortar cubes and edges fail to bear the pressure. Salahuddin et al. [56] reported that 300^0C is the temperature at which vertical cracks on concrete surfaces were developed. Figure 12-c and Figure 14-c, a full-length horizontal top edge failure and a large vertical crack along the full depth of the sample have been seen. On comparing the pattern of the cracks under elevated temperature, it can be conveniently concluded that up to 200°C maintains the sample's rigidity.

The failure mode of samples tested after the freezing and crushed ice-cooling cycle is shown in Figures 12, 13, 14-e and 14-f. However, the sample after freezing does not show any irregular pattern; samples in crushed ice-cooling show severe damage under failure load. In crushed ice-cooling mortar samples, particles started floating off the sample cubes, and outer boundary failure was also detected. Figures 12 and 14-f side edge chipping of samples was seen, and the bottom was disturbed. Figure 13-f shows the substantial crack pattern in the sample. Perpendicular cracks were developed, and some mortar was scattered due to the crushed ice water effects.

4. Conclusions

This study investigates sustainable cement sand mortar performance after incorporating solid wastes such as stone dust, crumb rubber, and silica fume with desert sand. The three sustainable mortar mixes, M1, M2, and M3, were studied. The performance of mixes was evaluated at ambient and elevated temperatures of 100°C, 200°C, and 300°C. Furthermore, mixes were studied under freezing and crushed ice-cooling temperatures (-10 ± 2°C) and (0 to -5°C), respectively. The following conclusions are drawn from the data obtained:

- The sustainable mortar combination M3 (50%NDS + 45%SD + 5%CR + (10%SF by weight of OPC)) showed the best performance under heating-cooling conditions. Based on analysis, it has been observed that silica fume helps in increasing strength when exposed to varying thermal conditions.
- The maximum mortar strength of M3 was (11.288 MPa) at 200°C. It was close to the recommended Type S value (12.4 MPa).
- All samples showed a minimum compressive strength under ice-crushed water. The mix M3 failed at (7.833 MPa) and did not meet the criterion of Type S (12.4 MPa). Even in ice-crushed water, the mix M3 successfully obtained a strength greater than the recommended Type N (5.2 MPa) and Type O (2.4 MPa) values.
- It has been concluded through the crack pattern that the rigidity is maintained in the samples up to 200°C. Large vertical cracks and edge failures were observed when the temperature was raised to a maximum of 300°C.
- In all mixes at 300°C, an unexpected color change was seen from dark grey solid to light yellow. The present study concluded that 300°C is a critical temperature to know mass loss behavior in developed sustainable mortar.
- Severe damages were identified in the samples under crushed ice water.

5. List of Abbreviations

AT	Ambient Temperature	M2	Natural Dune Sand Stone Dust Crumb Rubber Mortar
CR	Crumb Rubber	M3	Natural Dune Sand Stone Dust Crumb Rubber Silica Fume Mortar
FR	Freezer	OPC	Ordinary Portland Cement
IC	Crushed ice-cooling	SF	Silica Fume
NDS	Natural Dune Sand	SD	Stone Dust
M1	Natural Dune Sand Mortar		

6. Declarations

6.1. Author Contributions

Conceptualization, M.N.A. and D.A.H.M.; methodology, K.A.B.H.; software, M.N.A.; validation, M.N.A., D.A.H.M., and K.A.B.H.; formal analysis, M.N.A.; investigation, D.A.H.M.; resources, M.N.A.; data curation, D.A.H.M.; writing—original draft preparation, M.N.A.; writing—review and editing, K.A.B.H.; visualization, D.A.H.M.; supervision, A.I.H.M.; project administration, A.I.H.M.; funding acquisition, A.I.H.M. All authors have read and agreed to the published version of the manuscript.

6.2. Data Availability Statement

The data presented in this study are available in the article.

6.3. Funding

Fahad Bin Sultan University covered the article processing charge for this manuscript.

6.4. Conflicts of Interest

The authors declare no conflict of interest.

7. References

[1] Bendixen, M., Best, J., Hackney, C., & Iversen, L. L. (2019). Time is running out for sand. Nature, 571(7763), 29–31. doi:10.1038/d41586-019-02042-4.

[2] Best, J. (2019). Anthropogenic stresses on the world's big rivers. Nature Geoscience, 12(1), 7–21. doi:10.1038/s41561-018-0262-x.

[3] Torres, A., Brandt, J., Lear, K., & Liu, J. (2017). A looming tragedy of the sand commons. Science, 357(6355), 970–971. doi:10.1126/science.aao0503.

[4] Koehnken, L., & Rintoul, M. (2018). Impacts of sand mining on ecosystem structure, process and biodiversity in rivers. World Wildlife Fund International, Vaud, Switzerland.

[5] Seif, E. S. S. A., & Sedek, E. S. (2013). Performance of cement mortar made with fine aggregates of dune sand, Kharga Oasis, Western Desert, Egypt: an experimental study. Jordan Journal of Civil Engineering, 7(3), 270-284.

[6] Abu Seif, E. S. S., Sonbul, A. R., Hakami, B. A. H., & El-Sawy, E. K. (2016). Experimental study on the utilization of dune sands as a construction material in the area between Jeddah and Mecca, Western Saudi Arabia. Bulletin of Engineering Geology and the Environment, 75(3), 1007–1022. doi:10.1007/s10064-016-0855-9.

[7] Akhtar, M. N., Ibrahim, Z., Bunnori, N. M., Jameel, M., Tarannum, N., & Akhtar, J. N. (2021). Performance of sustainable sand concrete at ambient and elevated temperature. Construction and Building Materials, 280, 122404. doi:10.1016/j.conbuildmat.2021.122404.

[8] Akhtar, M. N., Jameel, M., Ibrahim, Z., Muhamad Bunnori, N., & Bani-Hani, K. A. (2023). Development of sustainable modified sand concrete: An experimental study. Ain Shams Engineering Journal, 102331. doi:10.1016/j.asej.2023.102331.

[9] Akhtar, M. N., Jameel, M., Ibrahim, Z., & Bunnori, N. M. (2022). Incorporation of recycled aggregates and silica fume in concrete: an environmental savior-a systematic review. Journal of Materials Research and Technology, 20, 4525–4544. doi:10.1016/j.jmrt.2022.09.021.

[10] Akhtar, M. N., Al-Shamrani, A. M., Jameel, M., Khan, N. A., Ibrahim, Z., & Akhtar, J. N. (2021). Stability and permeability characteristics of porous asphalt pavement: An experimental case study. Case Studies in Construction Materials, 15, 591. doi:10.1016/j.cscm.2021.e00591.

[11] Akhtar, M., Halahla, A., & Almasri, A. (2021). Experimental study on compressive strength of recycled aggregate concrete under high temperature. SDHM Structural Durability and Health Monitoring, 15(4), 335–348. doi:10.32604/sdhm.2021.015988.

[12] Nadeem Akhtar, M., & Tarannum, N. (2019). Flyash as a Resource Material in Construction Industry: A Clean Approach to Environment Management. Sustainable Construction and Building Materials, IntechOpen, London, United Kingdom. doi:10.5772/intechopen.82078.

[13] de Andrade Salgado, F., & de Andrade Silva, F. (2022). Recycled aggregates from construction and demolition waste towards an application on structural concrete: A review. Journal of Building Engineering, 52, 104452. doi:10.1016/j.jobe.2022.104452.

[14] Nisar Akhtar, J., Ahmad Khan, R., Ahmad Khan, R., Nadeem Akhtar, M., & Thomas, B. S. (2023). A comparative study of strength and durability characteristics of concrete and mortar admixture by bacterial calcite precipitation: A review. Materials Today: Proceedings. doi:10.1016/j.matpr.2023.03.490.

[15] Akhtar, M. N., & Akhtar, J. N. (2018). Suitability of Class F Flyash for Construction Industry: An Indian Scenario. International Journal of Structural and Construction Engineering, 12(9), 892–897.

[16] Jagadeep, R., Vignesh, R. V., Sumanth, P., Sarathi, V., & Govindaraju, M. (2021). Fabrication of fly-ash based tiles using liquid phase sintering technology. Materials Today: Proceedings, 46, 7224-7229. doi:10.1016/j.matpr.2020.12.348.

[17] Akhtar, M. N., Bani-Hani, K. A., Akhtar, J. N., Khan, R. A., Nejem, J. K., & Zaidi, K. (2022). Flyash-based bricks: an environmental savior—a critical review. Journal of Material Cycles and Waste Management, 24(5), 1663–1678. doi:10.1007/s10163-022-01436-3.

[18] Ahmad, S., Baghabra Al-Amoudi, O. S., Khan, S. M. S., & Maslehuddin, M. (2022). Effect of silica fume inclusion on the strength, shrinkage and durability characteristics of natural pozzolan-based cement concrete. Case Studies in Construction Materials, 17, 1255. doi:10.1016/j.cscm.2022.e01255.

[19] Prasad Bhatta, D., Singla, S., & Garg, R. (2022). Experimental investigation on the effect of Nano-silica on the silica fume-based cement composites. Materials Today: Proceedings, 57, 2338–2343. doi:10.1016/j.matpr.2022.01.190.

[20] Thomas, B. S., Gupta, R. C., Mehra, P., & Kumar, S. (2015). Performance of high strength rubberized concrete in aggressive environment. Construction and Building Materials, 83, 320–326. doi:10.1016/j.conbuildmat.2015.03.012.

[21] Wong, S. F., & Ting, S. K. (2009). Use of recycled rubber tires in normaland high-strength concretes. ACI Materials Journal, 106(4), 325–332. doi:10.14359/56652.

[22] Bani-Hani, K. A., & Senouci, A. (2015). Using waste tire crumb rubber as an alternative aggregate for concrete pedestrian blocks. Jordan Journal of Civil Engineering, 9(3), 400–409. doi:10.14525/jjce.9.3.3080.

[23] Algin, H. M., & Turgut, P. (2008). Cotton and limestone powder wastes as brick material. Construction and Building Materials, 22(6), 1074–1080. doi:10.1016/j.conbuildmat.2007.03.006.

[24] Ahmad Khan, R., Nisar Akhtar, J., Ahmad Khan, R., & Nadeem Akhtar, M. (2023). Experimental study on fine-crushed stone dust a solid waste as a partial replacement of cement. Materials Today: Proceedings. doi:10.1016/j.matpr.2023.03.222.

[25] Aïtcin, P.C. (1983). Condensed silica fume. Université de Sherbrooke, Sherbrooke, Canada.

[26] ACI 234R-96. (2000). Guide for the use of silica fume in concrete. American Concrete Institute (ACI), Michigan, United States.

[27] Asgeirsson, H., & Gudmundsson, G. (1979). Pozzolanic activity of silica dust. Cement and Concrete Research, 9(2), 249–252. doi:10.1016/0008-8846(79)90031-0.

[28] Saba, A. M., Khan, A. H., Akhtar, M. N., Khan, N. A., Rahimian Koloor, S. S., Petru, M., & Radwan, N. (2021). Strength and flexural behavior of steel fiber and silica fume incorporated self-compacting concrete. Journal of Materials Research and Technology, 12, 1380–1390. doi:10.1016/j.jmrt.2021.03.066.

[29] Akhtar, J. N., Khan, R. A., Khan, R. A., Akhtar, M. N., & Nejem, J. K. (2022). Influence of Natural Zeolite and Mineral additive on Bacterial Self-healing Concrete: A Review. Civil Engineering Journal (Iran), 8(5), 1069–1085. doi:10.28991/CEJ-2022-08-05-015.

[30] Pastore, G., Baird, T., Vermeesch, P., Resentini, A., & Garzanti, E. (2021). Provenance and recycling of Sahara Desert sand. Earth-Science Reviews, 216, 1–19. doi:10.1016/j.earscirev.2021.103606.

[31] Al-Harthi, A. A. (2002). Geohazard assessment of sand dunes between Jeddah and Al-Lith, western Saudi Arabia. Environmental Geology, 42(4), 360–369. doi:10.1007/s00254-001-0501-z.

[32] ASTM C1240-20. (2020). Standard Specification Silica Fume Used in Cementitious Mixtures. ASTM International, Pennsylvania, United States. doi:10.1520/C1240-20.

[33] BS 3148. (1980) Methods of Test for Water for Making Concrete. British Standard Institution (BSI), London, United Kingdom.

[34] ASTM C128-22. (2023). Standard Test Method for Density, Relative Density (Specific Gravity), and Absorption of Fine Aggregate. ASTM International, Pennsylvania, United States. doi:10.1520/C0128-22.

[35] GSO 1914/2009. (2009). Properties of Ordinary Portland Cement Type 1. GCC Standardization Organization, Riyadh, Kingdom of Saudi Arabia.

[36] ASTM C136-06. (2015). Standard Test Method for Sieve Analysis of Fine and Coarse Aggregates. ASTM International, Pennsylvania, United States. doi:10.1520/C0136-06.

[37] ASTM C1437-20. (2020). Standard Test Method for Flow of Hydraulic Cement Mortar: C1437-01. ASTM International, Pennsylvania, United States. doi:10.1520/C1437-20.

[38] IS 5512. (1983). Specification for flow table for use in tests of hydraulic cements and pozzolanic materials. Bureau of Indian Standards, New Delhi, India.

[39] Suman, B. K., Singh, A. K., & Srivastava, V. (2016). Stone Dust as Fine Aggregate Replacement in Concrete: Effect on Compressive Strength. International Journal of Advances in Engineering and Emerging Technology, 7(4), 3–8.

[40] Israr, M. B., Shahzada, K., & Khan, S. W. (2016). Impact of Waste Marble Dust on the Sustainability of Cement Sand Mortar. National Institute of Urban Infrastructure and Planning, University of Engineering and Technology, Peshawar 3rd Conference on Sustainability in Process Industry (SPI-2016), 19-20 October, 2016, Peshawar, Pakistan.

[41] Lohani, T., Padhi, M., Dash, K., & Jena, S. (2012). Optimum utilization of quarry dust as partial replacement of sand in concrete. International Journal of Applied Science and Engineering Research, 1(2), 391–404. doi:10.6088/ijaser.0020101040.

[42] Kankam, C. K., Meisuh, B. K., Sossou, G., & Buabin, T. K. (2017). Stress-strain characteristics of concrete containing quarry rock dust as partial replacement of sand. Case Studies in Construction Materials, 7, 66–72. doi:10.1016/j.cscm.2017.06.004.

[43] ASTM C39/C39M-01. (2017). Standard Test Method for Compressive Strength of Cylindrical Concrete Specimens. ASTM International, Pennsylvania, United States. doi:10.1520/C0039_C0039M-01.

[44] Neville, A. M. (1995). Properties of concrete (Vol. 4). Longman, London, United Kingdom.

[45] Park, S., Lee, B., Kim, J., & Yun, D. (2002). Planting-Ability Valuation of Porous Concrete Using Industrial By-Products. Journal of the Korea Concrete Institute, 14(4), 623–629. doi:10.4334/jkci.2002.14.4.623.

[46] Lee, K. H., & Yang, K. H. (2016). Development of a neutral cementitious material to promote vegetation concrete. Construction and Building Materials, 127, 442–449. doi:10.1016/j.conbuildmat.2016.10.032.

[47] Li, S., Yin, J., & Zhang, G. (2020). Experimental investigation on optimization of vegetation performance of porous sea sand concrete mixtures by pH adjustment. Construction and Building Materials, 249, 118775. doi:10.1016/j.conbuildmat.2020.118775.

[48] Saxena, R., Gupta, T., Sharma, R. K., Chaudhary, S., & Jain, A. (2020). Assessment of mechanical and durability properties of concrete containing PET waste. Scientia Iranica, 27(1), 1–9. doi:10.24200/sci.2018.20334.

[49] Dehdezi, P. K., Erdem, S., & Blankson, M. A. (2015). Physico-mechanical, microstructural and dynamic properties of newly developed artificial fly ash based lightweight aggregate - Rubber concrete composite. Composites Part B: Engineering, 79, 451–455. doi:10.1016/j.compositesb.2015.05.005.

[50] ASTM C270-19ae1. (2019). Standard Specification for Mortar for Unit Masonry. ASTM International, Pennsylvania, United States. doi:10.1520/C0270-19AE01.

[51] ASTM C1329-03. (2017). Standard Specification for Mortar Cement. ASTM International, Pennsylvania, United States. doi:10.1520/C1329-03.

[52] Khoury, G. A., Anderberg, Y., Both, K., Fellinger, J., Høj, N., & Majorana, C. (2007). Fib bulletin 38: Fire design of concrete structures—materials, structures and modelling, state-of-the art report. Federation Internationale du Beton, Lausanne, Switzerland.

[53] Khoury, G. A. (1992). Compressive strength of concrete at high temperatures: A reassessment. Magazine of Concrete Research, 44(161), 291–309. doi:10.1680/macr.1992.44.161.291.

[54] Fadiel. (2014). Use of Crumb Rubber To Improve Thermal Efficiency of Cement-Based Materials. American Journal of Engineering and Applied Sciences, 7(1), 1–11. doi:10.3844/ajeassp.2014.1.11.

[55] Tang, Y., Feng, W., Feng, W., Chen, J., Bao, D., & Li, L. (2021). Compressive properties of rubber-modified recycled aggregate concrete subjected to elevated temperatures. Construction and Building Materials, 268, 121181. doi:10.1016/j.conbuildmat.2020.121181.

[56] Salahuddin, H., Nawaz, A., Maqsoom, A., Mehmood, T., & Zeeshan, B. Ul A. (2019). Effects of elevated temperature on performance of recycled coarse aggregate concrete. Construction and Building Materials, 202, 415–425. doi:10.1016/j.conbuildmat.2019.01.011.

[57] Pathak, N., & Siddique, R. (2012). Effects of elevated temperatures on properties of self-compacting-concrete containing fly ash and spent foundry sand. Construction and Building Materials, 34, 512–521. doi:10.1016/j.conbuildmat.2012.02.026.

[58] Fares, H., Noumowe, A., & Remond, S. (2009). Self-consolidating concrete subjected to high temperature. Mechanical and physicochemical properties. Cement and Concrete Research, 39(12), 1230–1238. doi:10.1016/j.cemconres.2009.08.001.